

Camptothecin can increase the infiltration of CD8+T cells in local rabbit VX2 liver tumor

Keywords: Camptothecin (CPT), HCC, CD8, HSP90AB1, VX2, TACE

Abstract

In recent studies, drugs such as camptothecin have been found to affect the local immune response of tumors, increasing local CD8+T cell infiltration and MHC I expression, and enhancing the efficacy of immunotargeted drugs such as programmed cell death protein 1 (PD-1). Therefore, we studied whether camptothecin could have a similar effect on local immune response in liver cancer. At present, transarterial chemoembolization (TACE) is the most commonly used treatment for patients with HCC, and the rabbit VX2 hepatocellular carcinoma (HCC) model is a widely recognized animal model for HCC intervention. Therefore, we evaluated the effect of camptothecin on the local immunity of HCC in the rabbit VX2 HCC model by performing TACE. We divided 24 New Zealand rabbits into 4 groups according to weight and other factors: control group, camptothecin alone treatment group, embolization group, and embolization combined with camptothecin treatment group. One week after surgery, we studied the changes in the size and local immune cell infiltration of the tumor, and found that camptothecin significantly increased local CD8+T cell infiltration in the tumor, and embolization combined with camptothecin significantly inhibited tumor growth. However, the mechanism by which camptothecin drugs affect the local immune response of tumors is still unclear. We further analyzed on the information available on camptothecin in the traditional Chinese medicine systems pharmacology database and found that camptothecin may elicit a relevant immune response by acting on heat shock protein 90 alpha family class B member 1 (HSP90AB1), which is consistent with the previously reported findings on the effect of Hsp90 on the local immune response of tumors. The structures of camptothecin and HSP90AB1 were further studied and preliminarily verified, and camptothecin was found to be a potential inhibitor of HSP90AB1.

Introduction

Primary liver cancer or hepatocellular carcinoma (HCC) is the seventh most frequently occurring cancer globally and the second most common cause of cancer-related mortality. The prognosis for HCC is poor worldwide, and hence, the morbidity and mortality rates are roughly equal. In 2018, the global incidence of HCC was estimated at 9.3 per thousand and the death rate was 8.5 per thousand¹. The prevalence of nonalcoholic fatty liver disease (NAFLD)/nonalcoholic steatohepatitis (NASH) is increasing and may soon surpass viral factors as the leading cause of HCC worldwide². With the emergence of immunotherapy for treating HCC, there has been an increasing interest in determining the best way to combine immunotherapy with local therapy³.

Camptothecin, a chemotherapeutic drug, has long been a focus of research in antitumor treatment. A recent study found that camptothecin drugs can enhance the antitumor immune response when used as an antitumor medicine in topoisomerase inhibitors topology I tecan (TPT) treatment of breast cancer cells and induce the secretion of danger-associated molecular patterns, triggering the activation of dendritic cells (DC) and cytokine production. TPT has been reported to inhibit tumor growth in tumor-bearing mice and is associated with the infiltration of

activated DC and CD8+ T cells⁴. Camptothecin and a common cyclooxygenase-2 inhibitor have been found to inhibit transcription activity, induce the production of NR4a factor, and exert synergistic antitumor effects. Gene inactivation or drug inhibition of NR4a releases the effector activity of CD8+ cytotoxic T cells and elicits a powerful antitumor immune response⁵. Immunohistochemical analysis showed CD8+ lymphocyte infiltration and dense macrophages expressing inducible nitric oxide synthase (iNOS) and interleukin-15 in the liver metastases of mice treated with the combination therapy⁶. The number of CD4+/CD8+ co-expressed lymphocytes was significantly higher than that in a normal donor in both the subgroups⁷. DS-8201a is a drug like camptothecin. It can activate the immune system and inhibit tumor growth in mice. DS-8201a increases MHC class I expression in tumor cells, increases the expression of DC-activated markers, and increases tumor infiltration of CD8+T cells, all of which support the importance of the antitumor effect of DS-8201a on the immune system. Therefore, DS-8201a can be considered an effective immune stimulant⁸. Topoisomerase 1 (Top1) inhibitors can enhance T cell-mediated cytotoxicity in tumor cells and enhance the efficacy of tumor immunotherapy⁹. However, the mechanism by which camptothecin enhances the local immune response in tumors is still unclear.

Transarterial chemoembolization (TACE) is a commonly administered treatment for patients with HCC¹⁰. Therefore, we studied the effect of camptothecin administration on the local immunity of HCC during TACE in a rabbit VX2 HCC model, which is commonly used in studies related to interventional therapy¹¹.

Because the underlying mechanism by which camptothecin drugs affect the local immune response in HCC is still unclear, we further analyzed a pharmacology database to screen the core targets of their action. We also studied the structure of camptothecin and the selected target protein, and predicted its site of action, which was verified in vitro.

Materials and methods

1. A total of 24 healthy male adult New Zealand rabbits weighing 3.5 to 4 kg were used in the study. To determine the effect of camptothecin on the immune response in VX2 HCC model in rabbits, a VX2 cell suspension was first injected into the thigh muscle of New Zealand rabbits for developing a tumor-burdened rabbit. A tumor growth of about 1 cm in diameter was achieved that lead to the death of all the rabbits, after which the VX2 tumor tissue was obtained, after which the necrotic tissue was partly removed. The tumors were cut into sections, each of which had a volume of more than 1 mm³. The incised tumor mass was implanted into the left liver of healthy New Zealand rabbits. After 10 days, 1.5T MRI(Siemens) examination was performed to determine whether the HCC model was successfully constructed. The rabbits with successful HCC development were randomly divided into 4 groups with 6 rabbits in each group. The control group was infused with 2 mL of normal saline via the superselection of a tumor-feeding artery. In the embolization-only group, the rabbit liver tumor was embolized with lipiodol until the embolization procedure was complete. In the camptothecin-only treatment group, 2 mL of dissolved camptothecin solution was used for perfusion treatment of the tumor. In the camptothecin + embolization group, 2 mL camptothecin solution was first infused into the tumor and then lipiodol was used to embolize the tumor until embolization was complete. All the New Zealand rabbits were sacrificed 14 days after the surgery, and the liver tumors were removed and fixed for

subsequent pathological analysis and the detection of CD8 expression in the tumor tissue. We also observed the effects of the different treatment methods on the tumor immune response. Blood samples were obtained 1 day before the surgery and 3, 7 and 14 days after the surgery to monitor the changes in the levels of alanine transaminase (ALT), aspartate aminotransferase (AST), and creatinine, and blood cells.

2. To explore the mechanism by which camptothecin affects the local immune response in HCC, the traditional Chinese medicine systems pharmacology (TCMSP) database¹² was used to identify the target genes of camptothecin, and Uniprot¹³ was used to convert the full name of the target genes into gene symbols. GeneCards, OMIM, TDD, PharmGkb, and DrugBank were used to search for HCC-related genes, and then the HCC-related genes from these 5 databases were combined. The genes targeted by camptothecin intersected with HCC-related genes. These intersected genes were analyzed using STRING¹⁴ to construct a protein interaction network, and the relationship between different genes was obtained. Those genes that had no correlation with other genes were removed from the network. Then, Cytoscape¹⁵ was used to screen the genes in the protein interaction network to identify the core genes in this network. These core genes were used to perform the molecular docking analysis of camptothecin. The gene symbols in the protein interaction network were converted into Entrez IDs, after which GO and KEGG enrichment analyses were performed to obtain the gene enrichment data in terms of different functions and pathways in the protein interaction network. The 2D structure of camptothecin was searched in the PubChem database¹⁶ and downloaded. The 2D structure was converted into a 3D structure using ChemOffice. The PDB database¹⁷ was used to download the 3D structure of heat shock protein 90 alpha family class B member 1 (HSP90AB1). Thereafter, PyMOL¹⁸ was used to delete the water molecule and small molecule ligand in the 3D structure. Autodocktools was used to process the structure of HSP90AB1 and determine the active site. Vina¹⁹ was used to perform the molecular docking analysis of camptothecin and HSP90AB1 structures to determine their binding relationship and the optimal binding location. The inhibitory effect of camptothecin on HSP90AB1 at this binding site was further validated at the enzyme level. We used the HSP90AB1 assay kit (BPS Bioscience) to evaluate the inhibitory effect of camptothecin on HSP90AB1 and determined the IC₅₀ of the inhibitory effect of camptothecin on HSP90AB1.
3. Statistical analysis was performed using GraphPad Prism Version 8.0.2 and R Version 4.0.3. Data were expressed as mean \pm standard deviation. Two-way analysis of variance was used to compare the maximum diameter of tumor necrosis and the tumor growth rates in different groups on day 7 after surgery. Two-way ANOVA was used to compare ALT and AST levels between the four groups at different time points. Two-way ANOVA was also used to compare CD8+T-cells between different groups at the same time point and between two time points within the same group. A *p*-value of <0.05 was considered statistically significant.

Results

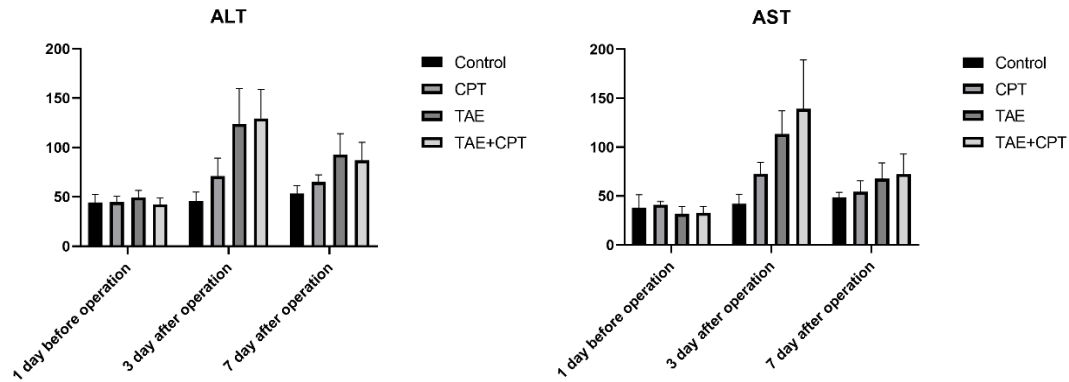


Figure 1. Changes of ALT and AST in rabbits.

The ALT and AST levels of the rabbits were measured 1 day before surgery, and 3 and 7 days after surgery. As shown in the figure, the liver function of the TACE and TACE+CPT groups 3 days after surgery was significantly worse than that of the control and CPT groups ($P < 0.05$). The liver function of the CPT group was slightly worse than that of the control group. Seven days after surgery, the liver function of the 3 treatment groups significantly improved ($P < 0.05$).

Table I. Tumor growth rate in different groups.

Group (n)	Tumor growth rate (%)	<i>P</i> value(compared with control group)
Control (6)	599.29 \pm 196.85	-
CPT (6)	421.66 \pm 267.38	>0.05
TAE (6)	208.54 \pm 131.42	0.0065
TAE+CPT (6)	93.04 \pm 60.40	0.0005

Ten days after the VX2 HCC rabbit model was established, the size and growth rate of the tumor increased 7 days after surgery, as shown in Table I. Tumor progression in the combined treatment group was the slowest ($P < 0.05$), whereas that in the control group was the fastest ($P < 0.05$), followed by the CPT- ($P < 0.05$) and embolization-only groups. The tumor growth rate of the combination therapy group was significantly slower than that of the CPT group ($P = 0.0243$).

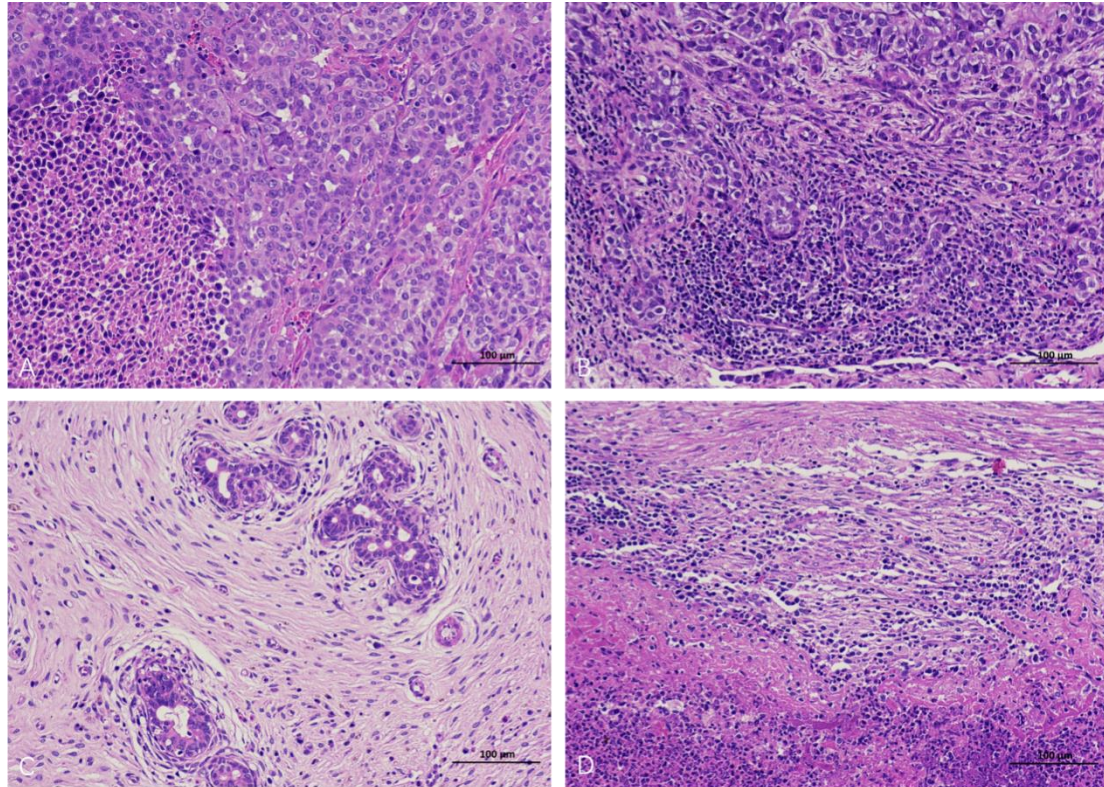


Figure 2. HE stained sections of tumor tissues in different groups.

In figure 2, A control group: the tumor had a high cytoplasmic ratio; clear mitosis; and vigorous cell proliferation. B Camptothecin-treated group: the tumor had a high nuclear to plasma ratio and mitotic images could be easily observed accompanied by diffuse lymphocyte infiltration. C. Embolization-only group: all tumor cells were necrotic and a large area of connective tissue was observed around the tumor accompanied by less lymphocyte infiltration. Local bile duct hyperplasia was also observed. D embolization + camptothecin treatment group: tumor cell nucleus to cytoplasm ratio was high; a large number of tumor cell necrosis could be seen locally; a large area of connective tissue hyperplasia could be seen in the tissue accompanied by diffuse lymphocyte infiltration.

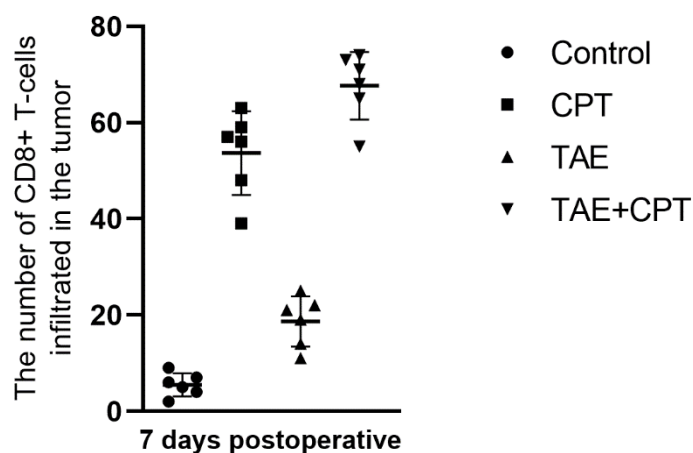


Figure 3. The number of CD8+ T cells infiltration in different groups seven days postoperative.

As was shown in figure 3, the number of CD8+T cells in the camptothecin-treated and camptothecin + embolization groups was significantly higher than that in the control and embolization-only groups ($P < 0.05$). Simple embolization could also slightly increase the infiltration of CD8+T cells in the tumor tissue ($P < 0.05$).

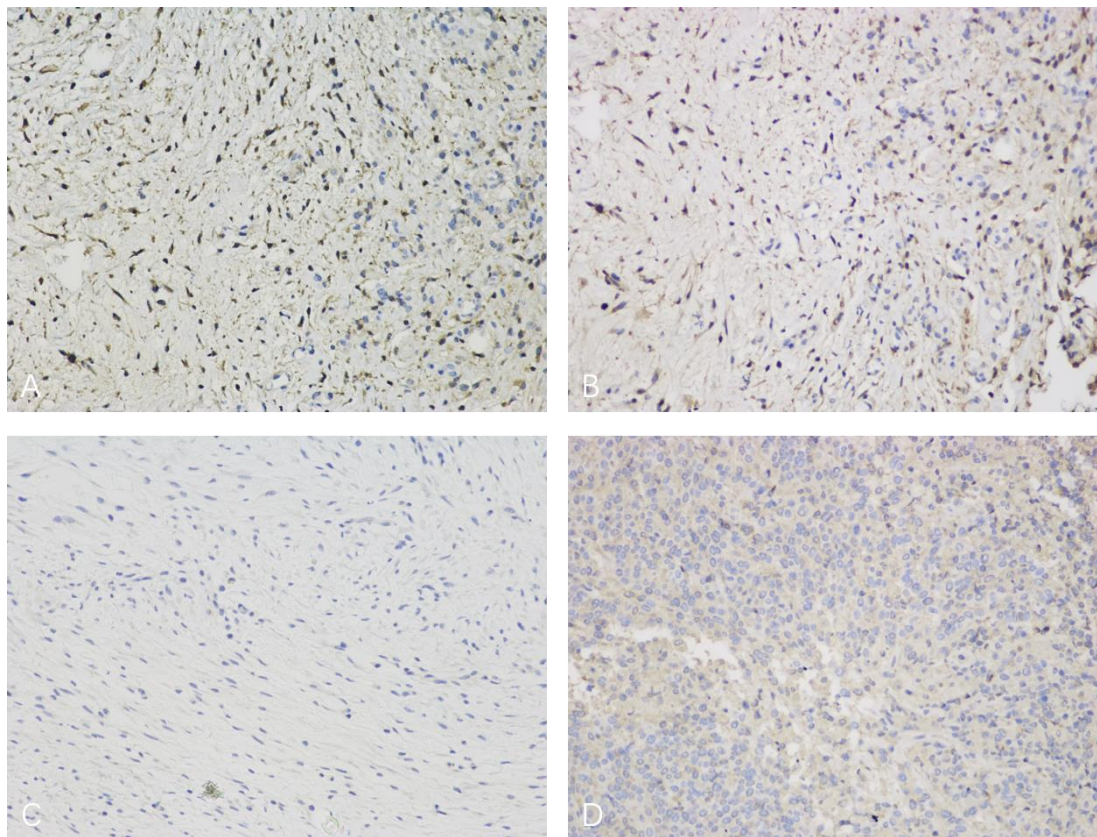


Figure 4. Immunohistochemical detection of CD8 in different groups.

Immunohistochemical detection of CD8 was shown in figure 4. A Camptothecin+embolization treatment group; B Camptothecin group; C Embolization-only group; D Control group. In the control group, tumor proliferation was strong, CD8+T cell infiltration was less in the embolization-only and control groups, whereas CD8+T cell infiltration significantly increased in the camptothecin-treated and camptothecin + embolization groups.

Table II. The targets of camptothecin in the TCMSP database

Drug	MolID	Symbol
Camptothecin	MOL009830	NOS2
Camptothecin	MOL009830	PTGS1
Camptothecin	MOL009830	KCNH2
Camptothecin	MOL009830	ESR1
Camptothecin	MOL009830	AR
Camptothecin	MOL009830	F10
Camptothecin	MOL009830	PTGS2
Camptothecin	MOL009830	F7
Camptothecin	MOL009830	KDR
Camptothecin	MOL009830	ACHE
Camptothecin	MOL009830	GSK3B

Camptothecin	MOL009830	HSP90AB1
Camptothecin	MOL009830	CDK2
Camptothecin	MOL009830	CHEK1
Camptothecin	MOL009830	PRKACA
Camptothecin	MOL009830	PRSS1
Camptothecin	MOL009830	PIM1
Camptothecin	MOL009830	CCNA2

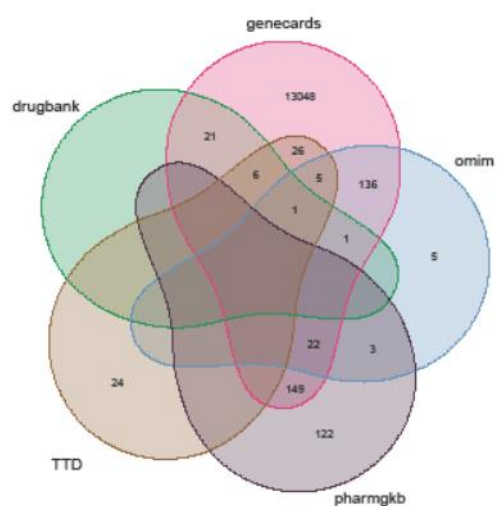


Figure 5. Venn diagrams of targets related to HCC in different databases.

In the table II, we have listed the main target genes of camptothecin according to our analysis of the information obtained from the TCMSP database¹². The figure 5 shows HCC-related genes identified in GeneCards, OMIM, TDD, PharmGkb and DrugBank. The number of intersected genes is shown in the Venn diagram.

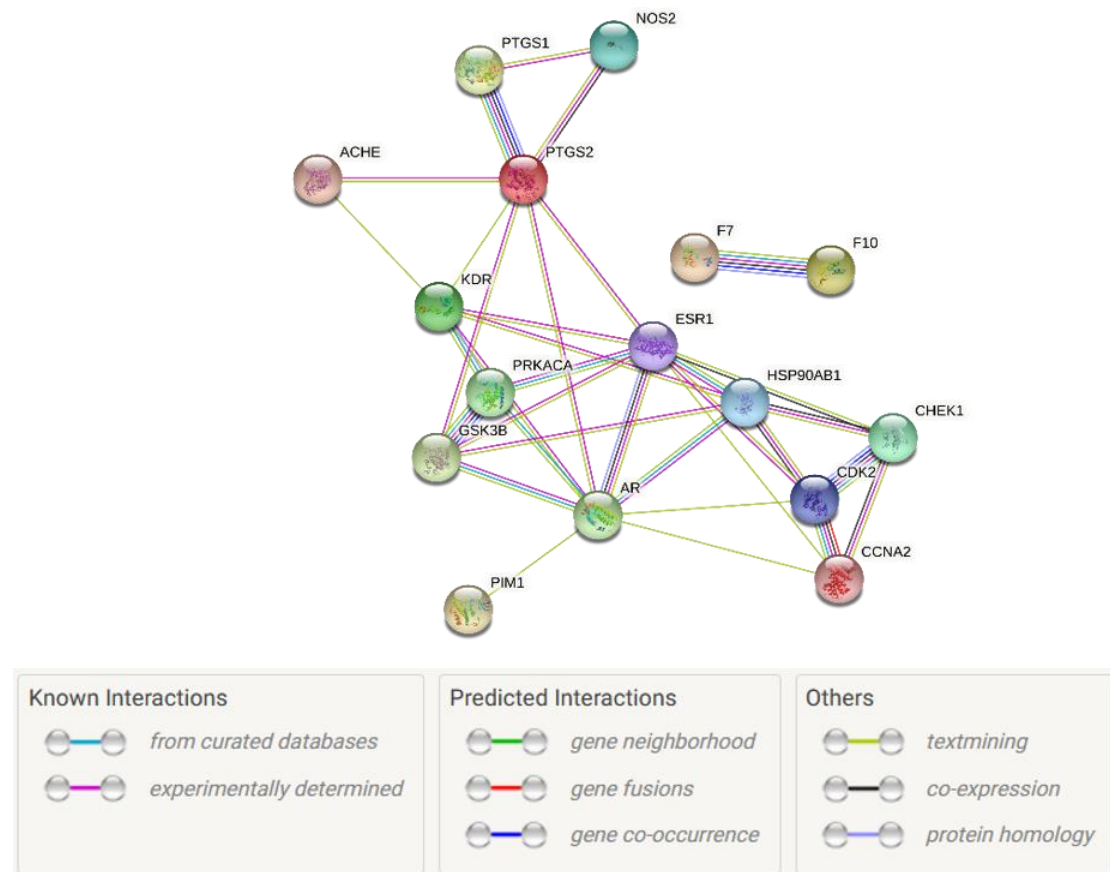


Figure 6. The protein interaction network of the intersection of camptothecin targets and HCC-related genes.

The HCC-related genes that intersected with the camptothecin-targeted genes were used to construct a protein interaction network(Figure 6), and the different relationships among these genes were connected by colorful lines.

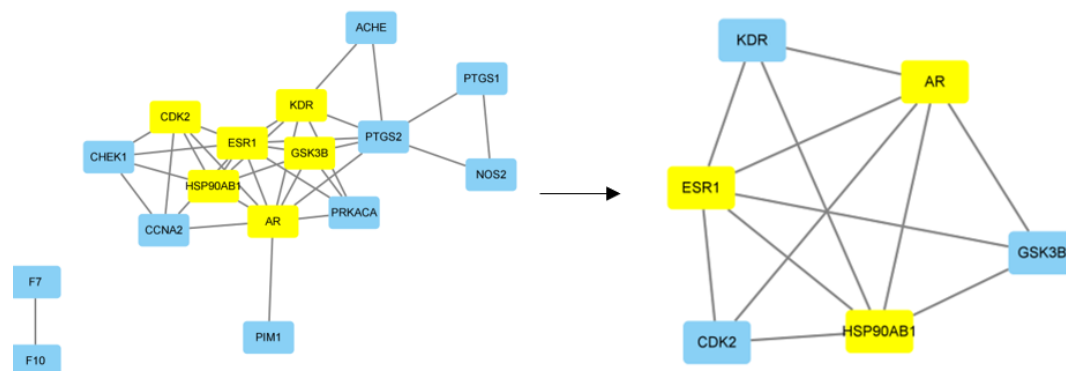


Figure 7. Screening the core genes of protein interaction network in Cytoscape.

The constructed protein interaction network was imported into Cytoscape¹⁵ to calculate the number of connections each gene has to other genes, and the core genes of the protein interaction network were identified by screening the genes according to the score(Figure 7). After screening the genes twice in the protein interaction network, those encoding AR, ESR1, and HSP90AB1—the core genes of the protein interaction network—were identified, which are shown in yellow.

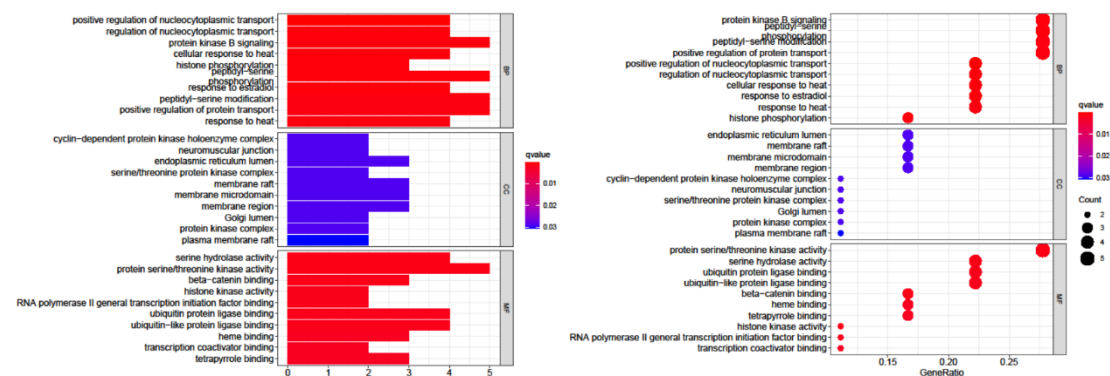


Figure 8. GO enrichment analysis of protein interaction network genes.

GO enrichment analysis of the protein interaction network genes was performed, and the results are shown in figure 8. These genes were significantly enriched in the following functions: positive regulation of nucleocytoplasmic transport, protein kinase B signaling, cellular response to heat, histone phosphorylation, peptidyl-serine phosphorylation, response to estradiol, peptidyl-serine modification, positive regulation of protein transport, serine hydrolase activity, protein serine/threonine kinase activity, beta-catenin binding, histone kinase activity, RNA polymerase II general transcription initiation factor binding, ubiquitin protein ligase binding, ubiquitin-like protein ligase binding, heme binding, transcription coactivator binding, and tetrapyrrole binding.

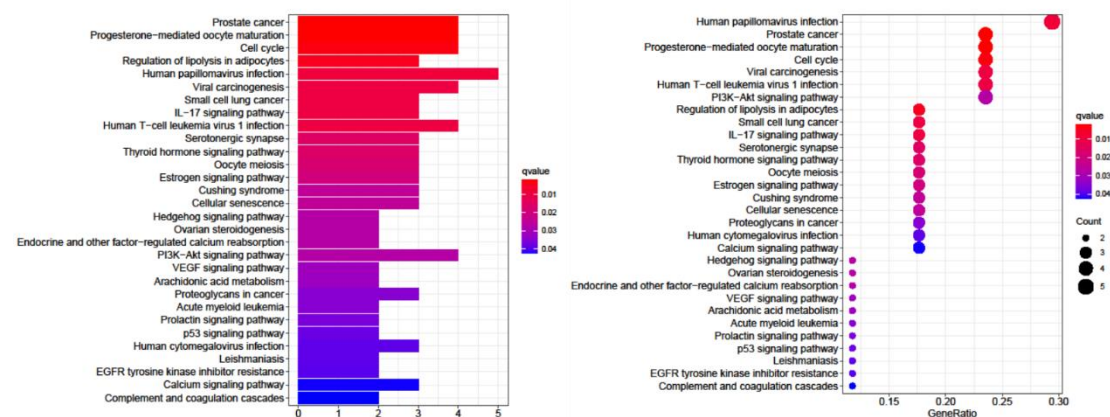


Figure 9. KEGG enrichment analysis of the protein interaction network genes.

KEGG enrichment analysis of the protein interaction network genes was performed, and the results are shown in figure 9. These genes were significantly enriched in the following events and conditions: prostate cancer, progesterone-mediated oocyte maturation, cell cycle, regulation of lipolysis in adipocytes, human papillomavirus infection, viral carcinogenesis, small cell lung cancer, IL-17 signaling pathway, and human T-cell leukemia virus 1 pathway.

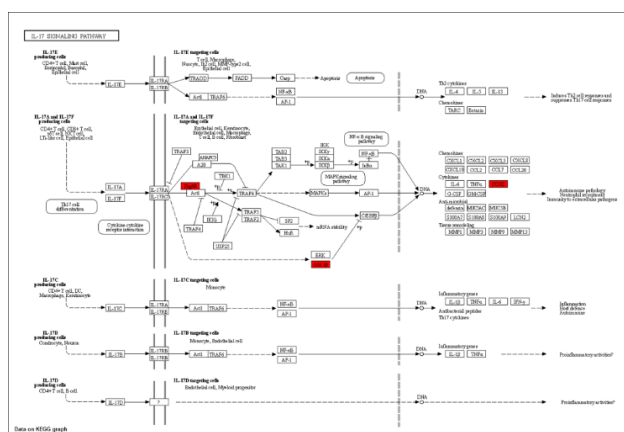


Figure 10. IL-17 signaling pathway.

The KEGG enriched IL-17 signaling pathway related to immune response was mapped, and the Hsp90, GSK3 β , and COX2 genes enriched in the IL-17 signaling pathway are marked in red in the above figure.

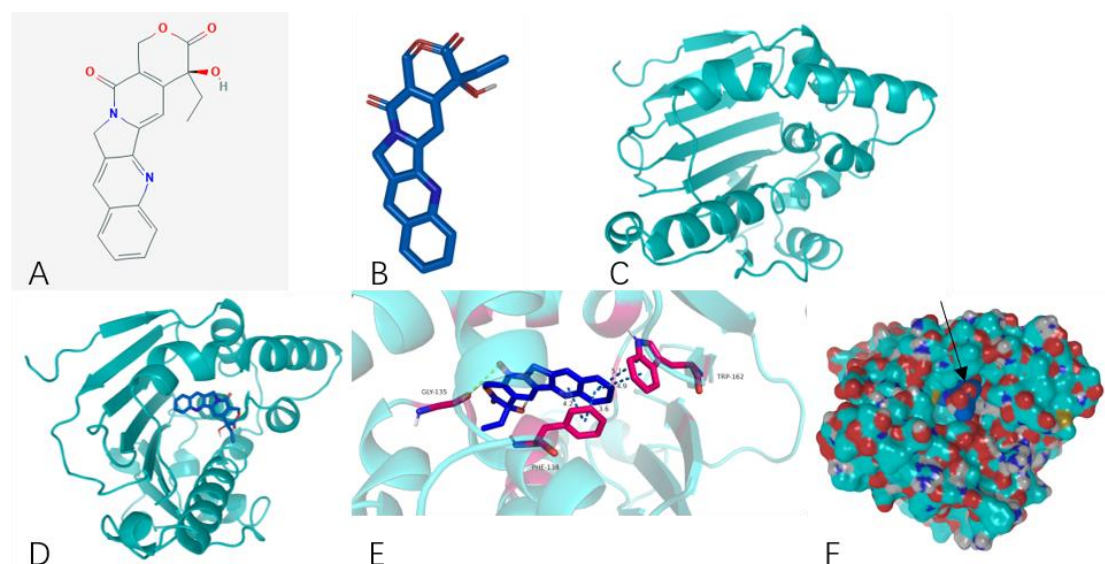


Figure 11. Schematic diagram of the structure of the combination of camptothecin and HSP90AB1.

The 2D structure of camptothecin (figure 11A) was downloaded and converted into a 3D structure (figure 11B). The 3D structure of HSP90AB1 (figure 11C) was also downloaded from PDB (3NMJ) and optimized. Then, the optimal binding site was found between camptothecin and the HSP90AB1 protein (figure 11D), which was located at the ATP-binding site. The binding free energy of camptothecin and HSP9AB1 was -9.2 kcal/mol, which was calculated in PyMOL. Camptothecin binds to HSP90AB1 through hydrogen bond (yellow) and pi-pi interaction (blue), as were shown in Figure 11E. The spatial structure of the binding of camptothecin and HSP90AB1 was shown in Figure 11F, and the arrow indicates the binding site of them.

IC50 screening of test compounds on HSP90AB1

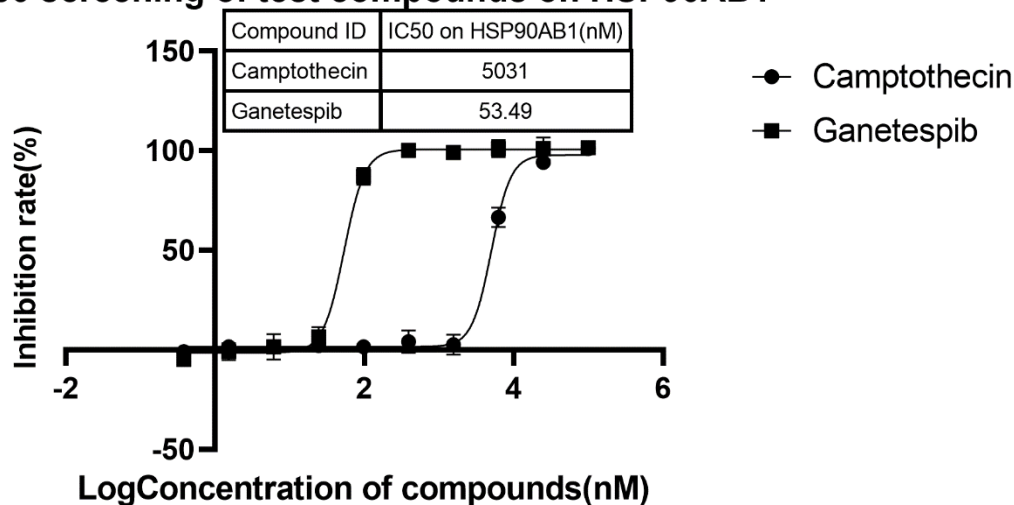


Figure 12. IC50 screening of camptothecin and ganetespib on HSP90AB1.

Take the logarithm of the compound concentration and perform non-linear regression analysis to obtain the IC50 of the inhibitory effect of camptothecin and ganetespib on HSP90AB1 (figure 12). As was shown in Figure 12, camptothecin had a weak inhibitory effect on HSP90AB1.

Discussion

Interventional embolization therapy is a commonly used clinical treatment for patients with HCC¹⁰, and it is considerably effective in patients with early HCC. However, poor efficacy of this therapy has been observed in a large number of patients. Recently, several types of tumor immunotherapies have emerged that can considerably improve the prognosis of some patients with HCC with less side effects but some patients are not sensitive to immunotherapy²⁰. Recent studies reported that camptothecin drugs enhance tumor immunotherapy, and the effect is relatively significant⁴⁻⁹, whereas CD8+T cells are mainly responsible for killing tumors²¹. In the present study, we found that camptothecin increased local CD8+T cell infiltration in the rabbit VX2 HCC model (commonly used in interventional surgery), and camptothecin combined with embolization therapy significantly inhibited tumor growth. Moreover, the postoperative liver function of rabbits was damaged to a certain extent but it recovered 1 week after surgery in the dual-treatment group. Before this has to do with the role of drugs like camptothecin related research reports are similar, but due to the limitation of experimental conditions, we have no further evaluation and camptothecin joint immune targeted therapy of tumors in animals curative effect, camptothecin can only be a potentially drugs enhanced immunotherapy, but the specific efficacy needs further experiments to explore. This may play a role through the IL-17 signaling pathway. Although the rabbit VX2 tumor model used in our study is similar to human HCC²², some differences and limitations with regard to this animal model exist. To further explore the mechanism underlying the effect of camptothecin on local immune response in HCC, the TCMSP database, which is a network of pharmacologically active compounds, was screened to identify the core target genes of camptothecin. We found that HSP90 was a potential target of camptothecin, and the effect of an Hsp90 inhibitor on tumor immunotherapy was similar to that of camptothecin on tumor immunotherapy²³⁻²⁷. These observations confirmed our findings. We also analyzed the structures of camptothecin and HSP90AB1, a

subtype of HSP90. Then, we found that camptothecin may inhibit the function of the HSP90AB1 protein by binding to its ATP-binding site. We further validated the idea at the enzyme level. Camptothecin had a weak inhibitory effect on HSP90AB1, which may be due to the insufficient affinity of them. It is necessary to further improve the structure of camptothecin to enhance its inhibitory effect on HSP90AB1. In animal experiments, interventional therapy may increase the local tumor drug concentration to inhibit HSP90AB1 and increase local CD8+T cell infiltration. Limited by conditions, we did not further explore the inhibitory effect of camptothecin on HSP90AB1. Camptothecin is a potential inhibitor of HSP90AB1, and its inhibitory effect needs to be further explored. The effect of HSP90 inhibitors on tumor progression has been widely confirmed but their side effects have limited their application²⁸. Inhibitors targeting HSP90AB1 have great potential, which has been reported in recent studies²⁸.

Conclusion

We found that camptothecin can increase local CD8+T cell infiltration in the VX2 HCC model established in New Zealand rabbits. Moreover, camptothecin is a potential inhibitor of the HSP90AB1 protein, which may be the reason why camptothecin increased local CD8+T cell infiltration in this model. Further study is required to elucidate the underlying mechanism of action of camptothecin in HCC.

1. Rheinbay E, Nielsen MM, Abascal F, et al. Analyses of non-coding somatic drivers in 2,658 cancer whole genomes. *Nature*. Feb 2020;578(7793):102-111. doi:10.1038/s41586-020-1965-x
2. McGlynn KA, Petrick JL, El-Serag HB. Epidemiology of Hepatocellular Carcinoma. *Hepatology*. Jan 2021;73 Suppl 1:4-13. doi:10.1002/hep.31288
3. Greden TF, Mauda-Havakuk M, Heinrich B, Korangy F, Wood BJ. Combined locoregional-immunotherapy for liver cancer. *J Hepatol*. May 2019;70(5):999-1007. doi:10.1016/j.jhep.2019.01.027
4. Kitai Y, Kawasaki T, Sueyoshi T, et al. DNA-Containing Exosomes Derived from Cancer Cells Treated with Topotecan Activate a STING-Dependent Pathway and Reinforce Antitumor Immunity. *J Immunol*. Feb 15 2017;198(4):1649-1659. doi:10.4049/jimmunol.1601694
5. Hibino S, Chikuma S, Kondo T, et al. Inhibition of Nr4a Receptors Enhances Antitumor Immunity by Breaking Treg-Mediated Immune Tolerance. *Cancer Res*. Jun 1 2018;78(11):3027-3040. doi:10.1158/0008-5472.CAN-17-3102
6. Shinohara H, Bucana CD, Killian JJ, Fidler IJ. Intensified regression of colon cancer liver metastases in mice treated with irinotecan and the immunomodulator JBT 3002. *Journal of immunotherapy (Hagerstown, Md : 1997)*. May-Jun 2000;23(3):321-31. doi:10.1097/00002371-200005000-00005
7. Ferrari S, Rovati B, Cucca L, et al. Impact of topotecan-based chemotherapy on the immune system of advanced ovarian cancer patients: an immunophenotypic study. *Oncology reports*. Sep-Oct 2002;9(5):1107-13.
8. Iwata TN, Ishii C, Ishida S, Ogitani Y, Wada T, Agatsuma T. A HER2-Targeting Antibody-Drug Conjugate, Trastuzumab Deruxtecan (DS-8201a), Enhances Antitumor Immunity in a Mouse Model. *Mol Cancer Ther*. Jul 2018;17(7):1494-1503. doi:10.1158/1535-7163.MCT-17-0749
9. McKenzie JA, Mbofung RM, Malu S, et al. The Effect of Topoisomerase I Inhibitors on the Efficacy of T-Cell-Based Cancer Immunotherapy. *J Natl Cancer Inst*. Jul 1 2018;110(7):777-786.

doi:10.1093/jnci/djx257

10. Cammà C, Schepis F, Orlando A, et al. Transarterial chemoembolization for unresectable hepatocellular carcinoma: meta-analysis of randomized controlled trials. *Radiology*. Jul 2002;224(1):47-54. doi:10.1148/radiol.2241011262
11. Keller S, Chapiro J, Brangsch J, et al. Quantitative MRI for Assessment of Treatment Outcomes in a Rabbit VX2 Hepatic Tumor Model. *Journal of magnetic resonance imaging : JMRI*. Sep 2020;52(3):668-685. doi:10.1002/jmri.26968
12. Ru J, Li P, Wang J, et al. TCMSP: a database of systems pharmacology for drug discovery from herbal medicines. *Journal of cheminformatics*. 2014;6:13. doi:10.1186/1758-2946-6-13
13. UniProt: the universal protein knowledgebase. *Nucleic acids research*. Jan 4 2017;45(D1):D158-d169. doi:10.1093/nar/gkw1099
14. von Mering C, Huynen M, Jaeggi D, Schmidt S, Bork P, Snel B. STRING: a database of predicted functional associations between proteins. *Nucleic acids research*. Jan 1 2003;31(1):258-61. doi:10.1093/nar/gkg034
15. Shannon P, Markiel A, Ozier O, et al. Cytoscape: a software environment for integrated models of biomolecular interaction networks. *Genome research*. Nov 2003;13(11):2498-504. doi:10.1101/gr.1239303
16. Kim S, Chen J, Cheng T, et al. PubChem 2019 update: improved access to chemical data. *Nucleic acids research*. Jan 8 2019;47(D1):D1102-d1109. doi:10.1093/nar/gky1033
17. Copoiu L, Torres PHM, Ascher DB, Blundell TL, Malhotra S. ProCarbDB: a database of carbohydrate-binding proteins. *Nucleic acids research*. Jan 8 2020;48(D1):D368-d375. doi:10.1093/nar/gkz860
18. Martinez X, Krone M, Alharbi N, et al. Molecular Graphics: Bridging Structural Biologists and Computer Scientists. *Structure (London, England : 1993)*. Nov 5 2019;27(11):1617-1623. doi:10.1016/j.str.2019.09.001
19. Macari G, Toti D, Pasquadibisceglie A, Polticelli F. DockingApp RF: A State-of-the-Art Novel Scoring Function for Molecular Docking in a User-Friendly Interface to AutoDock Vina. *International journal of molecular sciences*. Dec 15 2020;21(24)doi:10.3390/ijms21249548
20. Bruni D, Angell HK, Galon J. The immune contexture and Immunoscore in cancer prognosis and therapeutic efficacy. *Nature reviews Cancer*. Nov 2020;20(11):662-680. doi:10.1038/s41568-020-0285-7
21. St Paul M, Ohashi PS. The Roles of CD8(+) T Cell Subsets in Antitumor Immunity. *Trends in cell biology*. Sep 2020;30(9):695-704. doi:10.1016/j.tcb.2020.06.003
22. Nass N, Streit S, Wybranski C, et al. Validation of VX2 as a Hepatocellular Carcinoma Model: Comparison of the Molecular Reaction of VX2 and HepG2 Tumor Cells to Sorafenib In Vitro. *Anticancer research*. Jan 2017;37(1):87-93. doi:10.21873/anticancer.11293
23. Bae J, Munshi A, Li C, et al. Heat shock protein 90 is critical for regulation of phenotype and functional activity of human T lymphocytes and NK cells. *J Immunol*. Feb 1 2013;190(3):1360-71. doi:10.4049/jimmunol.1200593
24. Mbofung RM, McKenzie JA, Malu S, et al. HSP90 inhibition enhances cancer immunotherapy by upregulating interferon response genes. *Nature communications*. Sep 6 2017;8(1):451. doi:10.1038/s41467-017-00449-z
25. Rao A, Taylor JL, Chi-Sabins N, Kawabe M, Gooding WE, Storkus WJ. Combination therapy with HSP90 inhibitor 17-DMAG reconditions the tumor microenvironment to improve recruitment

of therapeutic T cells. *Cancer Res.* Jul 1 2012;72(13):3196-206. doi:10.1158/0008-5472.CAN-12-0538

26. Shimp SK, 3rd, Chafin CB, Regna NL, et al. Heat shock protein 90 inhibition by 17-DMAG lessens disease in the MRL/lpr mouse model of systemic lupus erythematosus. *Cell Mol Immunol.* May 2012;9(3):255-66. doi:10.1038/cmi.2012.5

27. Haggerty TJ, Dunn IS, Rose LB, Newton EE, Kurnick JT. A screening assay to identify agents that enhance T-cell recognition of human melanomas. *Assay and drug development technologies.* Apr 2012;10(2):187-201. doi:10.1089/adt.2011.0379

28. Khandelwal A, Kent CN, Balch M, et al. Structure-guided design of an Hsp90 β N-terminal isoform-selective inhibitor. *Nature communications.* Jan 30 2018;9(1):425. doi:10.1038/s41467-017-02013-1